Measurement 237 (2024) 115072

Contents lists available at ScienceDirect

Measurement

journal homepage: www.elsevier.com/locate/measurement

A stereoscopic video computer vision system for weed discrimination in rice field under both natural and controlled light conditions by machine learning

Mojtaba Dadashzadeh [a], Yousef Abbaspour-Gilandeh [a,*], Tarahom Mesri-Gundoshmian [a], Sajad Sabzi [a], Juan Ignacio Arribas [b,c,d,*]

[a] Department of Biosystems Engineering, College of Agriculture and Natural Resources, University of Mohaghegh Ardabili, Ardabil, Iran
[b] Department of Electrical Engineering, University of Valladolid, 47011 Valladolid, Spain
[c] Castilla-Leon Neuroscience Institute, University of Salamanca, 37007 Salamanca, Spain
[d] Artificial Intelligence Center, University of Valladolid, 47011 Valladolid, Spain

ARTICLE INFO

Keywords:
Image processing
Meta-heuristic algorithms
neural network (NN)
Optimization
Stereo vision

ABSTRACT

A site-specific weed detection and classification system was implemented with a stereoscopic video camera to reduce the adverse effects of chemical herbicides in rice field. A computer vision and *meta*-heuristic hybrid NN-ICA classifier were used to accurately discriminate between two weed varieties and rice plants, under either natural light (NLC) or controlled light conditions (CLC). Preprocessing, segmentation, and matching procedures were performed on images coming from either right or left camera channels. Most discriminant features were selected from average, either arithmetic or geometric, images using a NN-PSO algorithm. Accuracy classification results with the stereo computer vision system under NLC were 85.71 % for the arithmetic mean (AM) and 85.63 % for the geometric mean (GM), test set. At the same time, accuracy classification results of the computer vision system under CLC reached 96.95 % for the AM case and 94.74 % for the GM case, being consistently higher than those under NLC.

1. Introduction

Weeds are undesirable field plants that typically reduce crop yields by a range of 10 to 95 % affecting the normal growth of agricultural crops (Young et al. [46]). Common methods of weed control include: (1) chemical control with the spraying of herbicide, and (2) mechanical control with weeding or removal of weeds. Among these methods, chemical control is preferred by farmers due to the convenience, quick implementation, great effectiveness, and low operating cost. The main problem with chemical method for weed control is the implementation process. In conventional methods, herbicides are applied throughout the field. That way, there is no control over the amount of herbicide sprayed as a function of weed density due to the lack of uniform growth and distribution of weeds on fields. Therefore, even weed-free areas are sprayed with herbicides, which not only leads to a high consumption of herbicides and increased costs, but also to environmental pollution, including underground aquifers.

The study main objectives follow next:

1. To implement and automatic high accuracy weed detection and classification system in rice field to be potentially used later in selective herbicide application with precision agriculture, both reducing the waste of product and limiting the potential contamination to land and water table underneath and using the most effective herbicide product for each weed type.
2. To measure advantages of using stereoscopic (binocular) camera vision (either arithmetic or geometric R-L channel mean) as compared to monocular (either R or L) ordinary camera vision.
3. To measure the difference in classification performance when comparing controlled light conditions (CLC, LED) and natural light conditions (NLC, sunlight).

The structure of the remainder of the paper follows: first, we perform some literature review; next we present our dataset material and methods applied to them, including stereoscopic imaging, processing steps for weed identification, feature extraction, selection of sub-optimal highly discriminant features, and classification; next results and

* Corresponding authors at: Department of Electrical Engineering, University of Valladolid, 47011 Valladolid, Spain (J.I. Arribas).
E-mail addresses: abbaspour@uma.ac.ir (Y. Abbaspour-Gilandeh), jarribas@tel.uva.es (J.I. Arribas).

https://doi.org/10.1016/j.measurement.2024.115072
Received 5 February 2024; Received in revised form 29 May 2024; Accepted 4 June 2024
Available online 12 June 2024

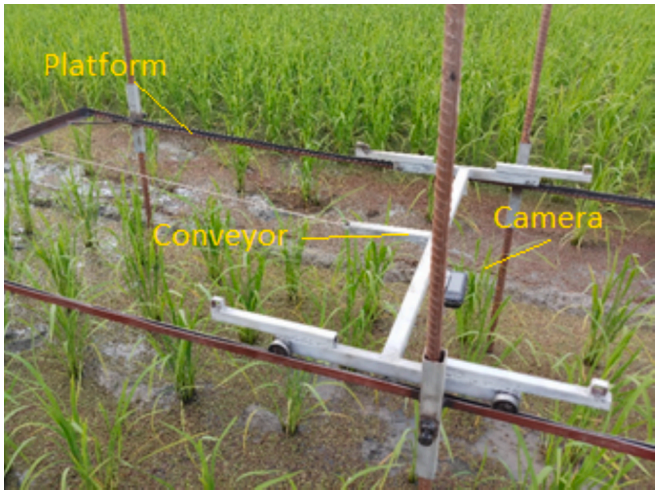

Fig. 1. Image of rail path built for imaging purposes in rice (R), Tarom-Fajr var., field: both rails and stereo camera are visible in picture (natural light conditions, NLC): about 2400–3000 lx (cd sr m^{-2}).

Fig. 2. Imaging under controlled light conditions (CLC) covering stereo video camera platform rails: artificial light was generated within the imaging space from a LED source with an illuminance of 460 lx (cd sr m^{-2}), approx.

discussion are presented, including the definition of effective discriminative features, ternary performance classification of rice and two weed plants, Video frame classification examples under both NLC and CLC lighting conditions, proper numerical evaluation of classifier performance by the computation of ROC and precision-recall curves, as well as their corresponding AUC values; next we conclude and finally we provide Supplementary data in the Video camera recording dataset examples including both original and detected output recordings, for both arithmetic and geometric means, L, and R channels and both under NLC and CLC lighting conditions.

1.1. Literature review

In recent years, farmers' interest in reducing production costs, on the one hand, and pressure from international institutions to reduce chemical pesticide emissions and their environmental impacts, on the other, have led researchers to review and develop site-specific management of weeds as a strategy to optimize and reduce herbicide application [8,27,34,47,39,29,15,33,32]. Site-specific strategy treats only those areas that are infested with weeds and affect crop yield or quality, leaving areas free of weed unaltered. By the selective application of chemical herbicides in varying doses depending on the location of weed infestation, a balance can be reached between production efficiency and environmental impact of chemical pesticide application [7]. Implementation of such weed control systems requires accurate identification and location of weed types in crop fields. Based on research in this context, three methods have been used to identify weeds to date: airborne remote sensing, photodetector-based sensing, and machine-vision based sensing [25]. Nevertheless, weed identification algorithms and devices have been developed with high accuracy given the complex agricultural environment, wide variety of plant species, and their various growth stages [25], but we can conclude that despite great advances have been found in the literature, weed detection under natural light conditions remains as a challenging open problem today.

Nowadays, machine vision has been used to properly identify weeds [12,26,31,32,33]. Different ambient light conditions cause segmentation and classification algorithms to fail due to shadows, reflections, different contrast levels, etc. For that reason, various studies have used different methods to improve the performance of automatic algorithms under different lighting conditions. The studies of Tang et al. [38], Hamuda et al. [16], Yang et al. [44], and Bai et al. [4] have used different color spaces. However, the proposed color space models seem to vary depending on target plants, and none of the models is universally valid, since no specific color space can be used for all plants and ambient imaging conditions. Besides choosing the right color space model, several methods have been presented to reduce the effect of different light conditions, such as synchronizing the global histogram in the preprocessing phase to minimize the effect of brightness [35] or improving image processing algorithms [33,32]. Another idea to reduce the effect of varying brightness and/or contrast is to improve the image quality when acquiring the images. For this reason, most studies have been conducted under controlled or limited light conditions on a specific stage of plant growth, regardless of the change in the biological characteristics of weeds as a function of time [33,32].

Recent relevant advances in the field of measurement with computer vision techniques applied in agriculture, weed detection [6], in plant leaf analysis [30], image segmentation [14], leaf disease detection [11,13] identification, pest monitoring [49], and Vis/NIR spectroscopic pesticide monitoring [18] in crop field have been developed, including also rice cultivar quality evaluation measurements [48] and a rice harvester based on Vis RGB-D imaging [37], amongst others.

Stereoscopic (stereo) vision imaging has been previously used as an efficient method to study canopy structure/stage in several studies [5,28,41]. Andersen et al. [1] conducted studies to assess the possibility of computing the geometric properties of plant such as plant height and leaf area from stereoscopic images taken with binoculars on potted plants and showed that stereo vision can accurately determine those plant properties. Jin and Tang [19] used 3D images along with the extracted features from 2D images to assess corn plants at early growth stages. By processing depth images, the algorithm effectively identified corn plants with 96.7 % accuracy and in addition it also detected their central position.

Li and Tang [24] used a 3D camera to detect both broccoli and green beans under weedy field conditions. The developed system overcame problems caused by foliage cover and light changes. They used the features extracted from 2D and 3D images, such as the gradient of amplitude and depth image, surface curvature, amplitude percentile index, normal direction, and count of neighboring points in 3D space, to identify both types of plants. The results of this study showed 88.3 % and 91.2 % detection rates for broccoli and green bean leaves, respectively.

Dandrifosse et al. [9] presented several challenges and solutions related to the identification of plant structure under natural farm light conditions. They used leaf area, mean leaf angle, leaf angle distribution, and canopy height traits of winter wheat in their study. The images were taken in field using a stereo camera. Then, using a machine learning (ML) based algorithm and RGB and HSV color spaces, segmentation of soil and plant was performed under variable lighting conditions. The mean spike top height was measured in this study with an accuracy of 97.1 %. Leaf area estimation showed a root mean square error (RMSE) of

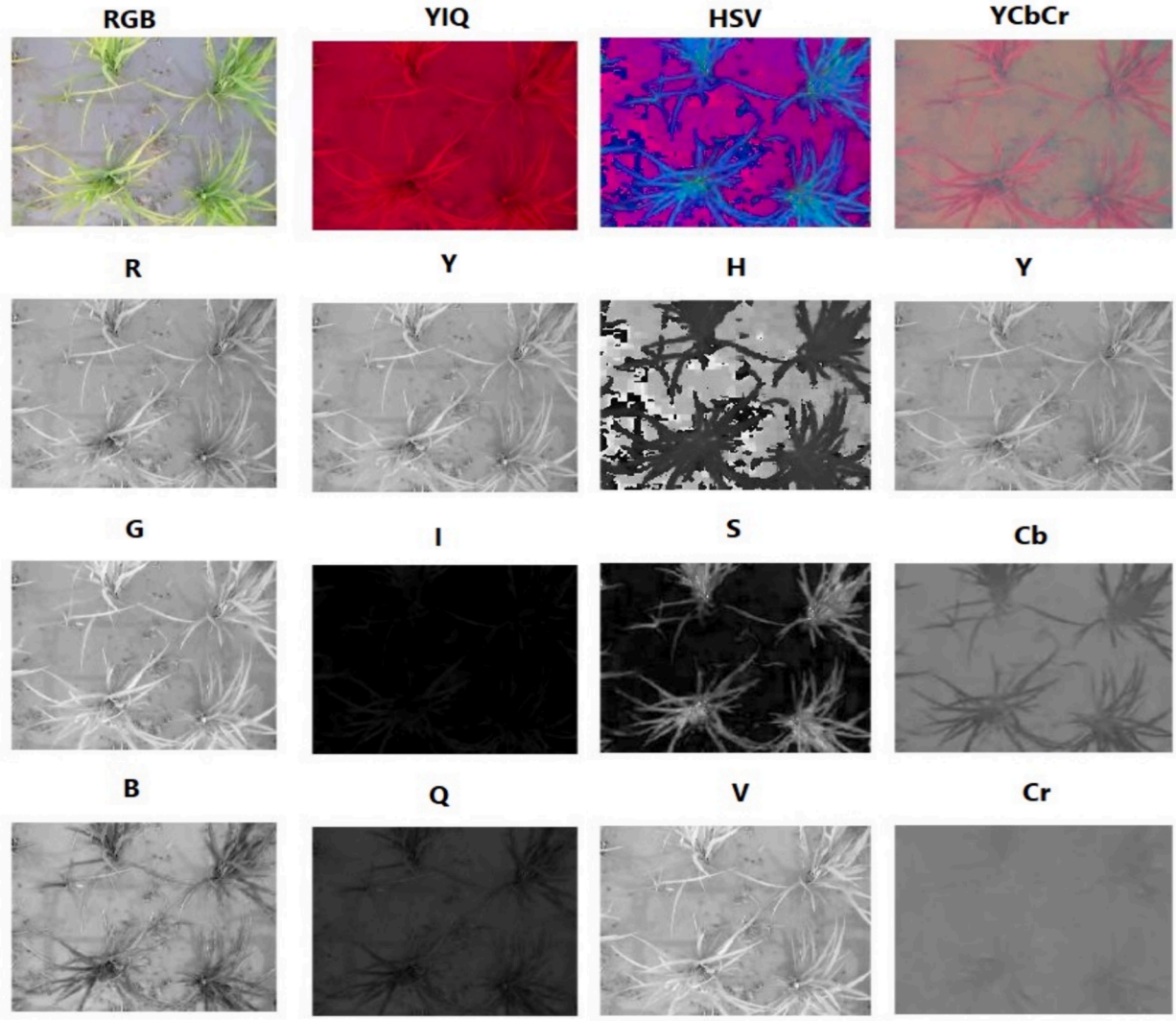

Fig. 3. Images from four of the most appropriate color spaces and their components under natural light conditions (NLC): RGB, YIQ, YCbCr, and HSV color spaces.

0.37 due to the effect of overlap between leaves. The mean leaf angle was calculated from 53° to 62° during the whole growing season. For each time point during the growing stage, the mean angle measurement varied less than 1.5 %, indicating that the method is accurate.

Dadashzadeh et al. [10] used a stereo vision system for distinguishing between rice and two types of weeds in a rice field by using machine learning techniques, comprising neural networks (NN) and two metaheuristic algorithms: a metaheuristic approach of particle swarm optimization (PSO) was used for selecting the most effective features and a bee algorithm (BA) was used to optimize the NN for accurately classifying rice plants from weeds. Research results showed an accuracy of about 90 % in stereo vison mode using an automatic classification algorithm.

Kamath et al. [20] used a deep learning-based semantic segmentation method for detecting and identifying two types of weeds from paddy crop and showed promising results with an accuracy over 90 %. In recent years, deep learning algorithms, as a new area of ML, has been used in several agriculture applications and has been developed into powerful methods for image classification, object detection, and localization, resulting in effective weed detection [21,17].

At the same time, [22] presented an IoT-Fog computing equipped robotic system for the categorization of weeds and soy plants during both the hazy and normal season. Results show a 97 % accuracy in classifying weeds and crops under a hazy environment. Although deep learning methods have achieved good results in weed and crop classification, so-called traditional (shallow) ML methods need a small sample size, short training time and are believed to better generalize to the disjoint (empty intersection) test set. In addition, shallow ML have a lower requirement for graphic processing units [43], for obvious reasons.

Given it is often difficult to obtain appropriate information about rice plants, especially under real farm/field environment conditions with variable natural light intensity due to overlapping and shadows caused by vegetation density, this study attempted to use a new processing technique based on the information fusion coming from two separate sources (stereo images) together with a combination of artificial intelligence and metaheuristic algorithms to better distinguish weeds from rice plants. Moreover, extensive experiments were conducted to evaluate the performance of the proposed method under two lighting conditions: either natural light imaging or controlled light imaging.

2. Materials and methods

To discriminate rice crops from weeds in rice field, the high-yielding Tarom-Fajr rice (R) crop variety was imaged in Mazandaran, Iran (36°37′48.71″N, 52°30′11.39″E) in 2017 with two dominant weed plants: *Cyperus rotundus* (C), from *Cyperaceae* family, and *Echinochloa crus-galli* (E), from *Poaceae* family. The common method of rice

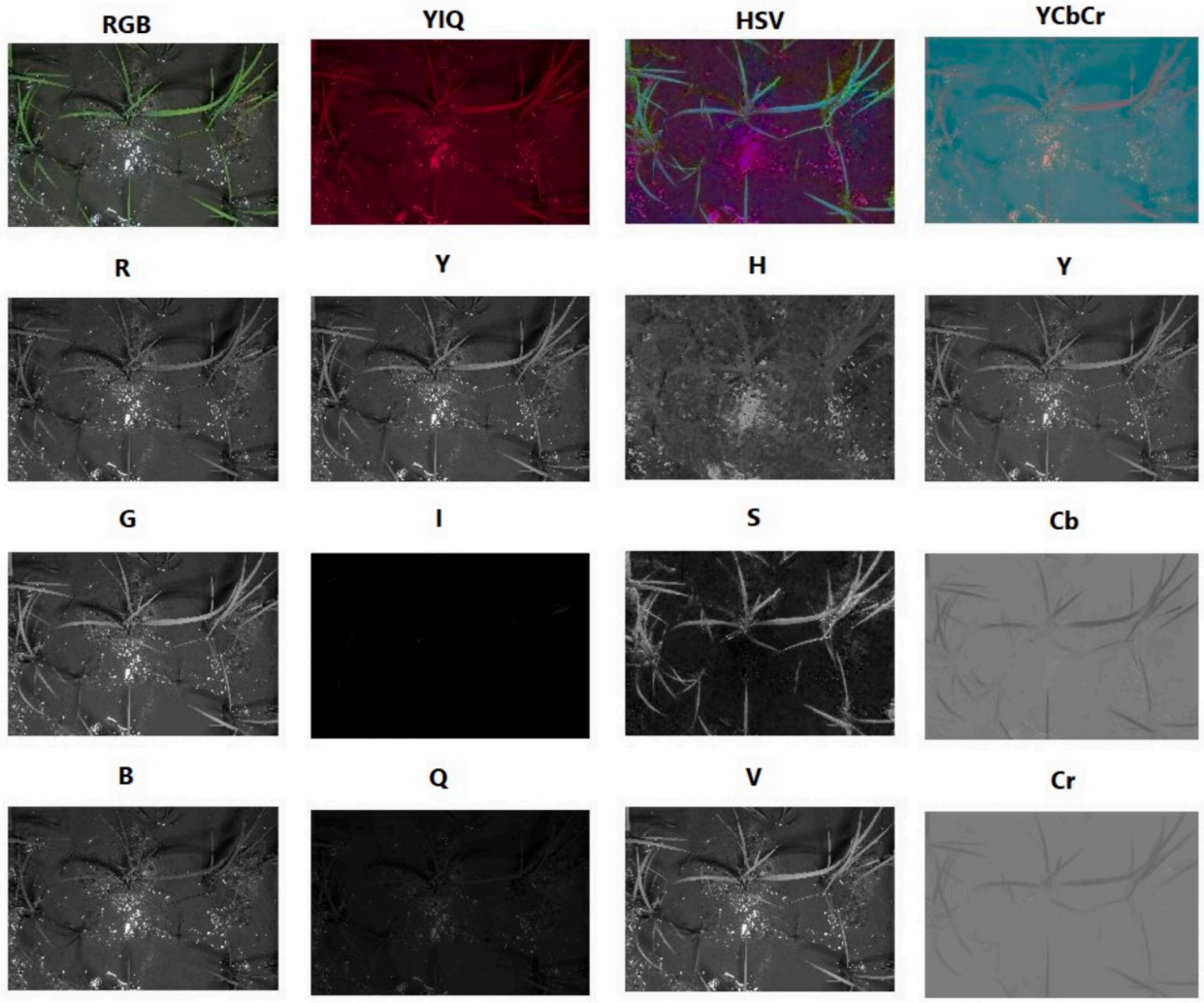

Fig. 4. Image samples from four of the most convenient color spaces and their elements under controlled light conditions (CLC): RGB, YIQ, YCbCr, and HSV color spaces.

cultivation in the region is traditional transplanting, which begins in mid-April. The traditional method for weed control was mainly chemical control in the form of drip spraying in field water in early stage of emerging weeds and spraying on weeds foliage after growth, together with manual (by hand) mechanical weeding. Besides the high consumption of herbicides, drip spraying (water-mixing method) is associated with massive environmental contamination. In addition, foliar spraying in rice fields is a costly method due to the need of a lot of herbicide application and might require great care because of the specific farm conditions. By taking advantage of intensive farming and intelligent spraying systems, the efficiency of this method is expected to be increased.

2.1. Stereoscopic imaging method

A stereoscopic digital camera (Fujifilm FinePix Real 3D-W3, Tokyo, Japan) equipped with a 10-megapixels CCD sensor recording stereo Videos in AVI format (NTSC), ISO 400 sensitivity, frame resolution of 480 × 440 pixels, 30 frames per second, was used for imaging under different light conditions. Data were collected as stereo Videos and finally the right (R) and left (L) channels of each 3D frame were extracted. To move the camera over the farm field, a rail platform was designed, and hand built, as shown in Fig. 1. The camera was moved at a height of 70 cm above the soil surface using a conveyor with the lowest vibration possible (approximately 30 cm from the top of plant leaf). The imaging process was performed over a length of three meters with a movement speed of 0.13 m/s approx. To create controlled light conditions, the entire path of the camera movement was covered with tarpaulin, to avoid sunlight to enter in the recording field. In addition, artificial light was generated within the imaging space from a LED source with an illuminance of approx. 460 lx (cd sr m^{-2}), as shown in Fig. 2. Data analysis was performed using MatLab software (Mathworks, Natick, MA) on a personal computer system equipped with an Intel Core i5-2540 m 2.6 GHz processor and 4 GB of RAM memory, running under a 64-bit operating system. The Videos were recorded during the third and fourth weeks after transplanting, when herbicide application reduces weed competition. Illuminance of natural light during imaging operations was about 2400–3000 lx (cd sr m^{-2}).

2.2. Processing steps to identify weeds

Almost all available methods for weed identification involve two main steps: 1) segmentation of vegetation against background (soil and/or residue) and computation of features from objects extracted after segmentation; 2) classification of plant pixels as either desired crop or undesired weed plants [40].

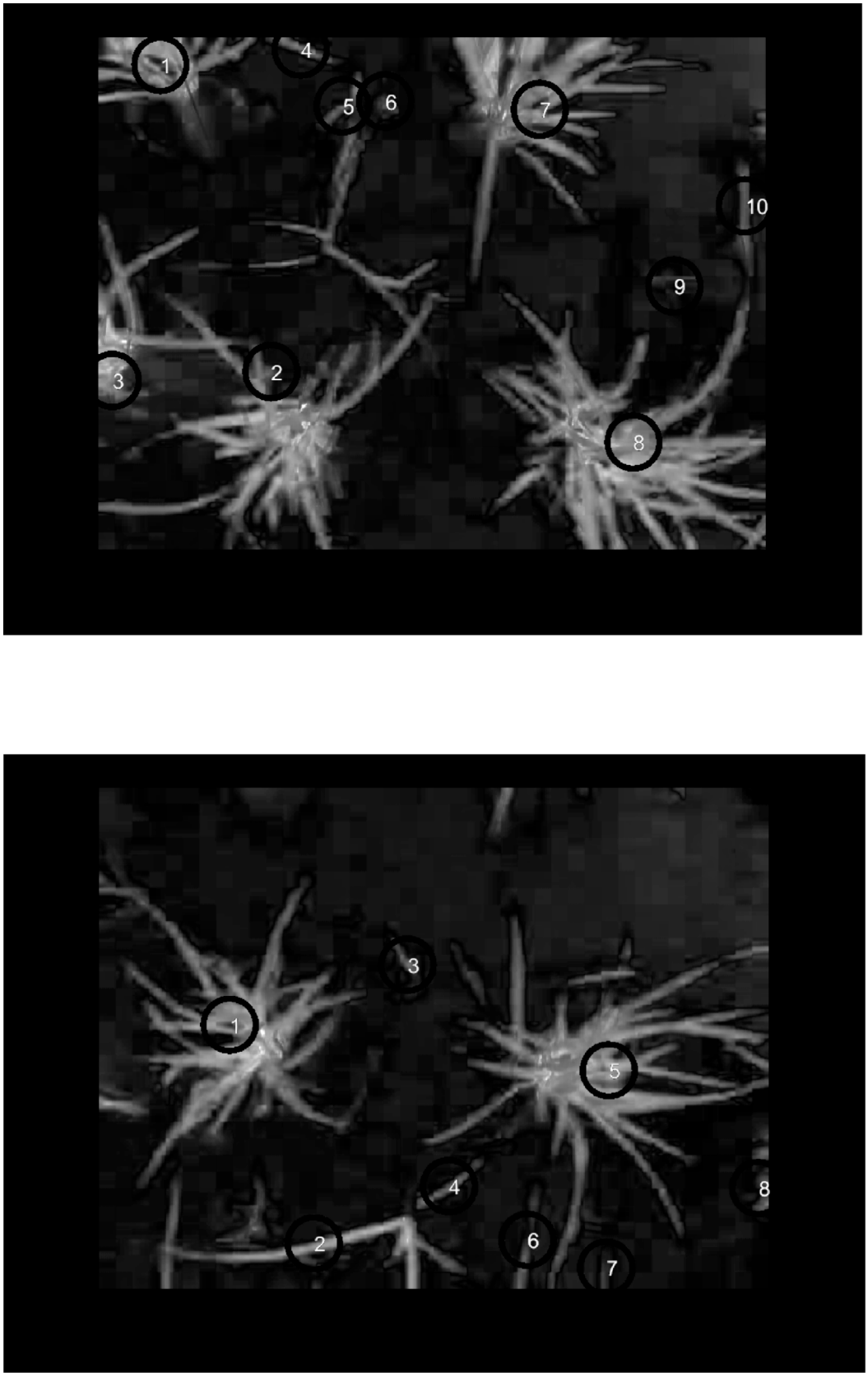

Fig. 5. Detection of the green components (weeds and rice crop) of sample video frames in the selected *S* channel under natural light conditions (NLC): two video frame examples are depicted; the numbers shown inside black circles in the sample video frames represent the number of green components extracted.

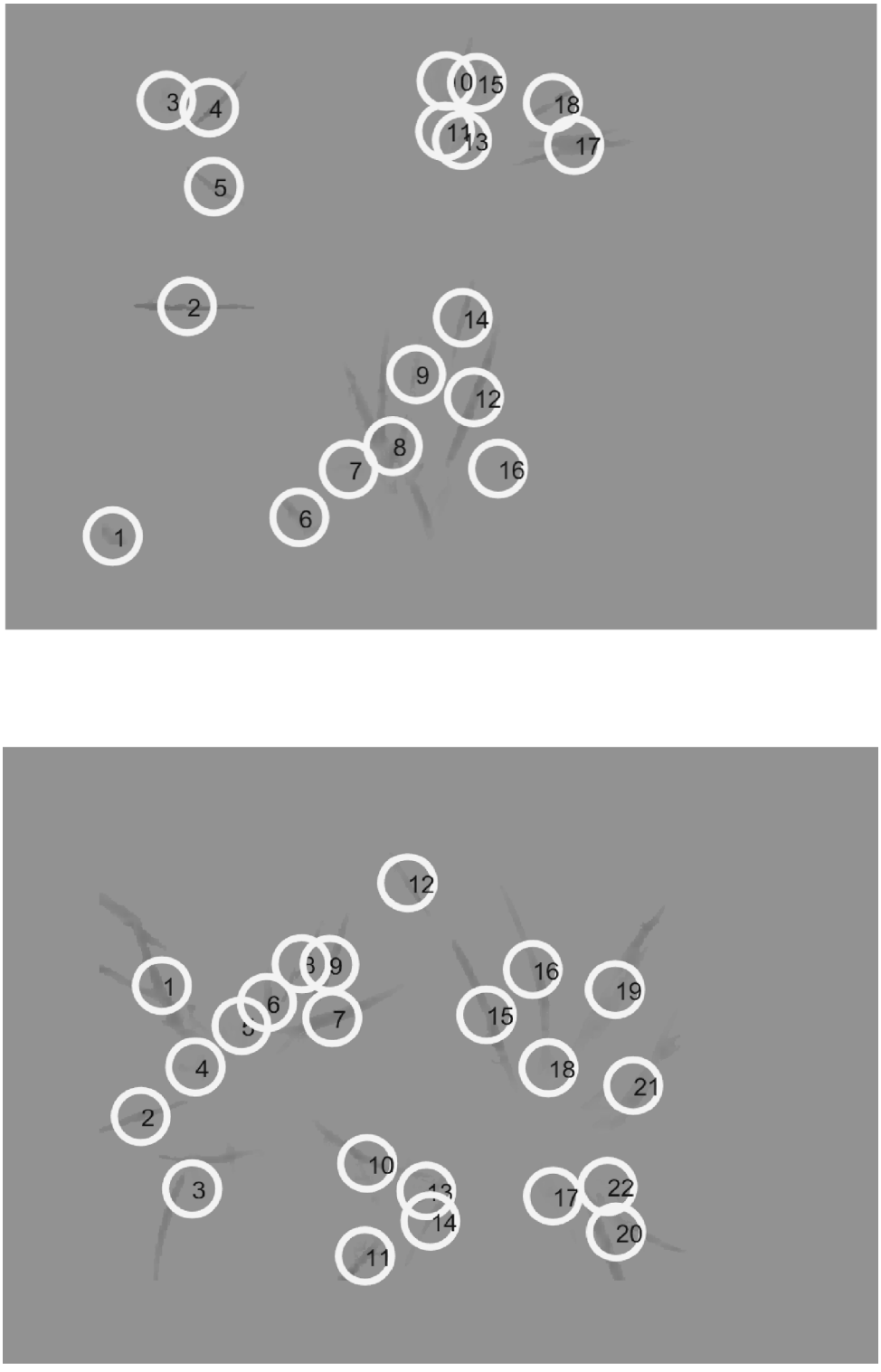

Fig. 6. Detection of the green components (weeds and rice crop) of sample video frames in the selected *Cb* channel under controlled light condition (CLC): two video frame examples are depicted; the numbers shown inside white circles in the sample video frames represent the number of green components extracted.

Table 1
NN-PSO Effective selected features under natural light conditions (NLC) for detecting weeds in high-yielding Fajr rice plant variety crop field.

Arithmetic Mean (AM)	ExH-HSV, CIVE- CMYY, correlation- 45°, correlation- 90°, variance- 90°, PTB
Geometric Mean (GM)	Gn-RGB, HV I-HSV, ExR-RGB, SS-HSV, information measure of correlation-135°, convexity

Table 2
NN-PSO Effective selected features under controlled light conditions (CLC) for detecting weeds in high-yielding Fajr rice plant variety crop field.

Arithmetic Mean (AM)	Difference entropy- 135°, correlation- 0°, correlation- 45°, RBI-RGB, GB-RGB, SRAD(5)
Geometric Mean (GM)	Sum entropy- 135°, contrast- 135°, Homogeneity- 0°, SANG (4), Std-H, B-avr

Table 3
Description of the effective discriminant features for detecting weeds in rice field: name and formal definitions.

Formal Description	Selected Feature Name
Excess Hue from HSV color space	ExH-HSV
Color index for extracted vegetation cover in CMY color space	CIVE-CMY
$N_g(i,j) = \frac{g(i,j)}{\sum_i \sum_j g(i,j)}$ $\text{Correlation} = \frac{\sum_i \sum_j (i-\mu_i)(j-\mu_j) N_g(i,j)}{\sigma_i \sigma_j}$	Correlation-X^0
Ration of Perimeter to Enclosing Rectangle	PTB
Gn = G/(R + G + B), (The normalized secend component of RGB)	Gn −RGB
$\text{HVI} = (H_n - V_n)/(H_n + V_n)$ $H_n = H/(H+S+V)$, $V_n = V/(H+S+V)$	HVI-HSV
$\text{EXR} = 1.4 \times R_n - G_n$	ExR-RGB
Average Saturation from HSV color space	SS-HSV
$\text{IMC} = \frac{ENT - HXY1}{max(Hx, Hy)}$ $HXY1 = -\sum_{i=0}^{n-1} \sum_{j=0}^{n-1} Ng(i,j) \ln[Nx(i).Ny(j)]$, $N_x(i) = \sum_{i=0}^{n-1} Ng(i,j)$, $N_y(j) = \sum_{j=0}^{n-1} Ng(i,j)'$, H_X: Entropy of N_x and H_y: Entropy of N_y	Information measure of correlation-X^0
A measure of the curvature	Convexity
$\text{Difference entropy} = -\Sigma p_{x-y}(i) ln[p_{x-y}(i)]$, $p_{x\text{-}y}(k) = \sum_{i,j:[i-j]=k} Ng(i,j) for k = 0, \cdots, N(g-1)$	Difference entropy-X^0
$\text{RBI} = (G_n - B_n)/(G_n + B_n)$ $B_n = B/(R+G+B)$	RBI-RGB
$GB = (G_n - B_n)$	GB-RGB
$m_{pq} = \sum_x \sum_y x^p y^q f(x,y) \text{p,q} = 0,1,2,\ldots$ $\eta_{pq} = \mu_{pq}/\mu'^{\gamma}_{00} p,q = 0,1,2,\cdots, \gamma = \frac{p+q}{2} + 1$ $p+q = 2,3,\cdots \phi_5 = [(\eta_{30} - 3\eta_{12})(\eta_{30} + \eta_{12})[(\eta_{30} + \eta_{12})^2 - 3(\eta_{21} + \eta_{03})^2] + (3\eta_{21} - \eta_{03})(\eta_{21} + \eta_{03})[3(\eta_{30} + \eta_{12})^2 - (\eta_{21} + \eta_{03})^2]$	SRAD (5) (moment invariants 5)
$p_{x+y}(k) = \sum_{i,j:i+j=k} N_g(i,j) for k = 2,3,\cdots,2L$ $\text{Sum Entropy} = -\sum_{i=2}^{2L} p_{x+y}(i) \log(p_{x+y}(i))$	Sum entropy-X^0
$N_g(i,j) = \frac{g(i,j)}{\sum_i \sum_j g(i,j)}$ $\text{Contrast} = \sum_i \sum_j (i-j)^2 N_g(i,j)$	Contrast- X^0
$\text{Homogeneity} = \sum_i \sum_j \frac{N_g(i,j)}{1+\lvert i-j \rvert}$	Homogeneity-X^0
$\phi_4 = (\eta_{30} + \eta_{12})^2 + (\eta_{21} + \eta_{03})^2$,	SANG (4) Difference of moment invariants-4
Standard deviation of Hue from HSV color space	Std-H
Average Blue from RGB color space	B-avr

2.2.1. Vegetation segmentation

Segmentation attempts to extract pixels belonging to vegetation from other components of the image were carried out. To achieve that goal, this study first performed preprocessing of the recorded images. Initially, the right (R) and left (L) channels of the stereo Video recorded over farm rice field were separated and the frames belonging to both channels were extracted by coding in MatLab software. Around 1250 Video frames were extracted from each recorded channel. Due to the

Table 4
Confusion matrix and percentage classification for test data in NLC stereo mode as arithmetic mean (AM): test set.

Predicted/Real class	Rice	*Cyperus r.*	*Echinochloa c-g*	Classification error (%)	Classification accuracy (%)
Rice	90	7	1	8.16	
Cyperus r.	5	48	11	25.00	85.71
Echinochloa c-g	4	17	34	38.18	

Table 5
Confusion matrix and percentage classification for test data in NLC stereo mode as geometric mean (GM): test set.

Predicted/Real class	Rice	*Cyperus r.*	*Echinochloa c-g*	Classification error (%)	Classification accuracy (%)
Rice	86	8	4	12.24	
Cyperus r.	4	45	15	29.68	85.63
Echinochloa c-g	5	10	40	27.18	

Table 6
Confusion matrix and percentage classification for test data in stereo mode as arithmetic mean (AM): test set.

Predicted/Real class	Rice	*Cyperus r.*	*Echinochloa c-g*	Classification error (%)	Classification accuracy (%)
Rice	65	3	5	10.95	
Cyperus r.	0	40	0	0	96.95
Echinochloa c-g	5	0	46	9.8	

Table 7
Confusion matrix and percentage classification for test data in stereo mode as the geometric mean (GM): test set.

Predicted/Real class	Rice	*Cyperus r.*	*Echinochloa c-g*	Classification error (%)	Classification accuracy (%)
Rice	64	4	5	12.32	
Cyperus r.	0	40	0	0	94.74
Echinochloa c-g	4	9	38	25.49	

Table 8
Confusion matrix and percentage classification for test data from left (L) channel of camera under controlled light conditions (CLC): test set.

Predicted/Real class	Rice	*Cyperus r.*	*Echinochloa c-g*	Classification error (%)	Classification accuracy (%)
Rice	63	6	4	13.69	
Cyperus r.	2	30	8	25	90.80
Echinochloa c-g	3	5	43	15.68	

Table 9
Confusion matrix and percentage classification for test data from right (R) channel of camera under controlled light conditions (CLC): test set.

Predicted/Real class	Rice	*Cyperus r.*	*Echinochloa c-g*	Classification error (%)	Classification accuracy (%)
Rice	63	7	4	14.68	
Cyperus r.	3	33	5	19.51	90.85
Echinochloa c-g	7	6	39	30.95	

sensitivity of segmentation and its effect on other subsequent stages of the machine vision system in distinguishing weeds from crop under different lighting conditions, an attempt was made to select color space for optimal segmentation purposes. For this reason, six color spaces, comprising RGB, HSV, YIQ, CMY, HSI, and YCbCr, and their respective channels were investigated, with resulting examples of four of the most appropriate color spaces under both natural light (NLC) and controlled light (CLC) conditions, shown in Figs. 3 and 4, respectively.

As shown in Fig. 3, the third channel (Q) of the YIQ color space and the second and third channels components (S, V) of the HSV and (Cb, Cr) of the YCbCr color spaces have good segmentation capabilities for imaging conditions under natural light, and after further testing with more images, the S channel was selected as the optimal segmentation channel under NLC. To judge from images in Fig. 4, the third channel (Q) of YIQ color space and the second and third channels (Cb, Cr) of YCbCr color space, again have good segmentation capabilities for imaging under CLC, and after further testing with additional images, the Cb channel was finally selected as the optimal segmentation channel under CLC. At the same time, Figs. 5 and 6 show sample frames on which the green components are segmented. The numbers shown inside circles in the sample Video frames represent the number of green components extracted.

Then, by examining different Video frames, a fixed segmentation threshold level of 125 was selected as the best threshold to separate image objects under NLC imaging conditions and a fixed segmentation threshold level of 180 was selected under CLC conditions. By separating plant parts from plant background (soil) and residue, the color, texture, and shape features of the segmented objects under both imaging conditions were extracted and passed to the classification algorithms to discriminate rice from weed plants. A total of 302 features were extracted from the segmented objects.

2.2.2. Feature extraction

After identifying plant pixels, weed detection using machine vision methods is usually done with a combination of information about color, position, shape, texture, size and/or spectrum of weeds and crops. The use of either only one or many features depends on how images are taken and the type of crop and weed species [7]. In this study, a total of 302 features comprising color, shape, and texture, were extracted for accurate discrimination of rice and weed plants, under both imaging conditions, either NLC or CLC. A total of 146 features were related to texture based on the co-occurrence matrix and histogram analysis, 127 color features were computed based on the average deviation and standard pixel values in each of the three channels of the six color spaces (RGB, HIS, HSV, YIQ, CMY, and YCbCr) and vegetation indices, and additional 29 shape features, were computed from each object. It should be noted that to extract shape features, the result of the segmentation had to be converted into binary images, a process that is always associated with the generation of unwanted noise and holes in the image. To solve this problem, a morphological closing operation was used to connect the broken thin components and fill in the small holes [36]. Also, a combination of dilation and erosion operations was used as a closing filter to smooth object's axes.

Based on research objectives – to achieve high accuracy in discriminating rice from weeds under both natural and controlled light conditions- after extracting the features from right and left image channels, the matching operations between the R and L channels corresponding points was performed. In order to take advantage of stereoscopic imaging, the arithmetic (AM) and geometric mean (GM) values between the corresponding points in R and L channels were computed, c.f. Eqs. (1) and (2). It should be noted that AM and GM are two mathematical concepts that usually differ in the method of calculation. The AM (or simply mean) is computed by adding all the numbers in the dataset and dividing the result by the total number of data points, while the GM is calculated by multiplying the numbers in the dataset and taking the n-th root from the result, where n is the total number of data points [45]. AM and GM values were computed according to the following formal equations:

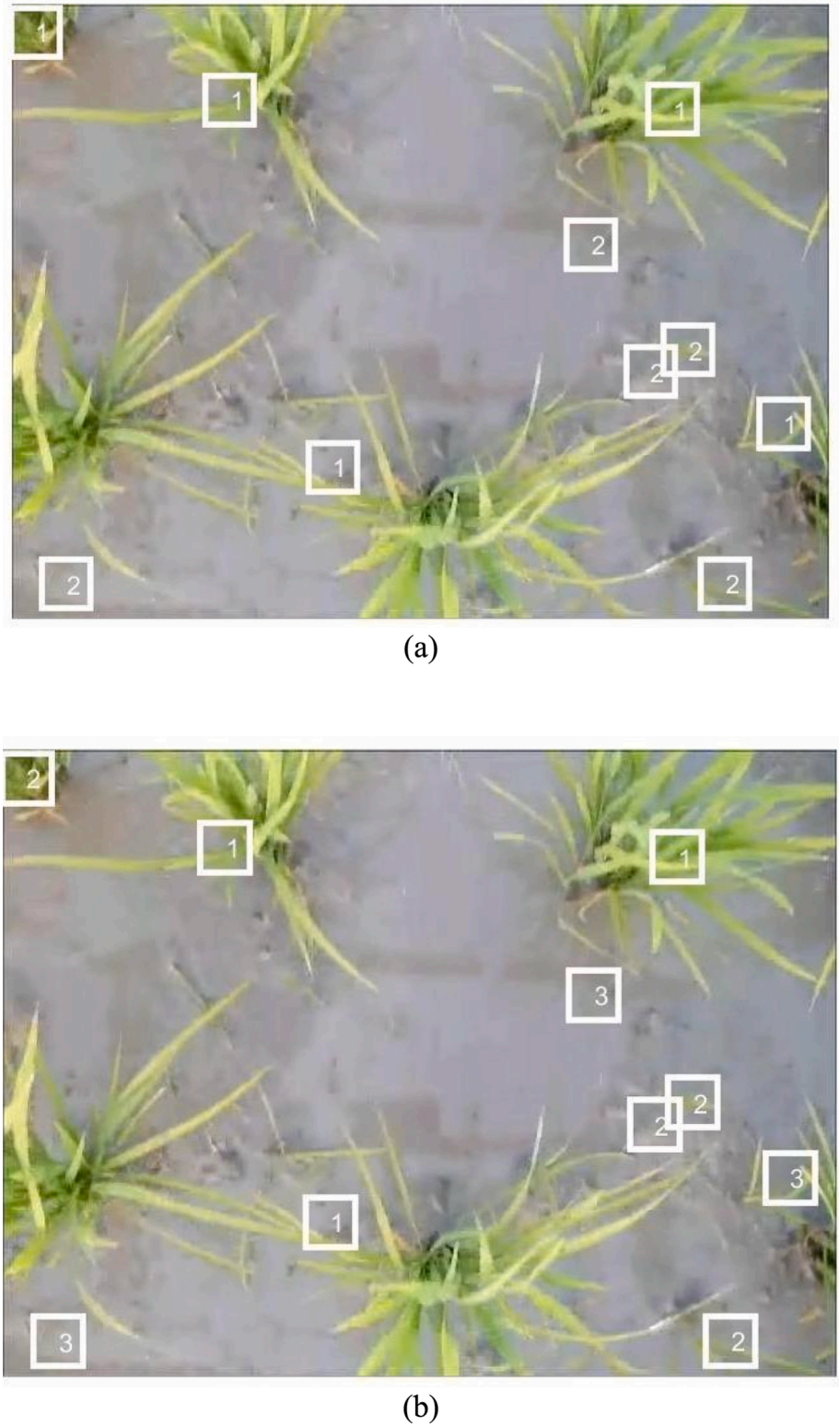

Fig. 7. Classification result under natural light conditions (NLC) for three plant classes: 1) rice plant (R), 2) *Cyperus rotundus* (C) weed, and 3) *Echinochloa* (E) *crus-galli* weed: (a) stereo video mode with arithmetic mean (AM) computation, frame extracted from **Arithmetic mean model_NLC.mp4** supplementary video file, and (b) stereo video mode with geometric mean (GM) computation, frame extracted from **Geometric mean model_NLC.mp4** supplementary video file.

$$\text{Arithmetic Mean (AM)} = \frac{\text{Right channel} + \text{Left channel}}{2} = \frac{\text{R} + \text{L}}{2} \quad (1)$$

$$\text{Geometric mean (GM)} = \sqrt{\text{Right channel} \times \text{Left channel}} = \sqrt{\text{RL}} \quad (2)$$

2.2.3. Selection of effective discriminant features

The various features extracted from images are not equally important and some of the features may even be considered as noise in the weed detection process. To increase the processing speed for pattern recognition and improve the classification accuracy, we tried to select the best

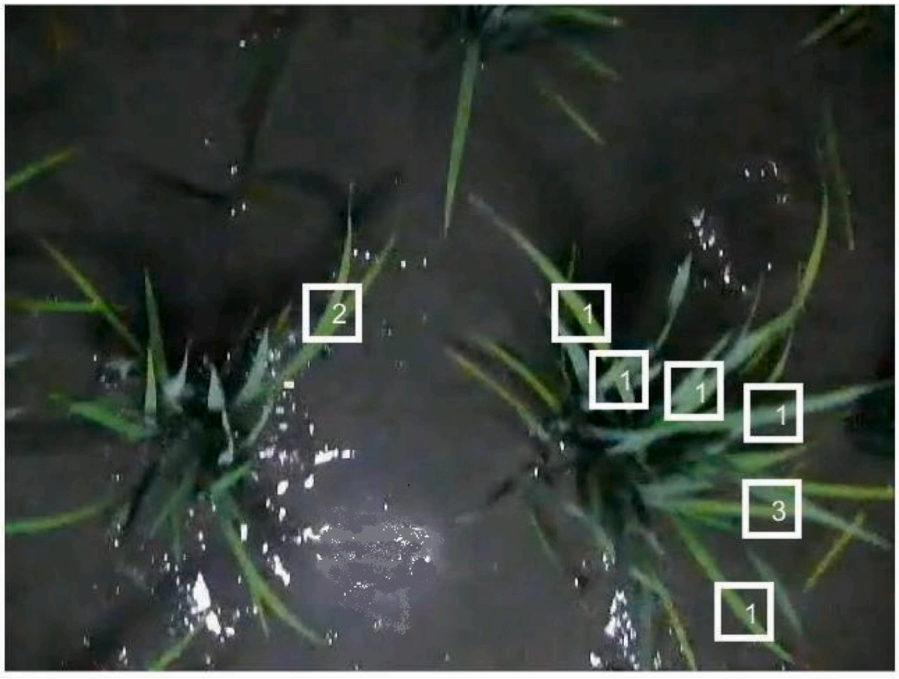

(a)

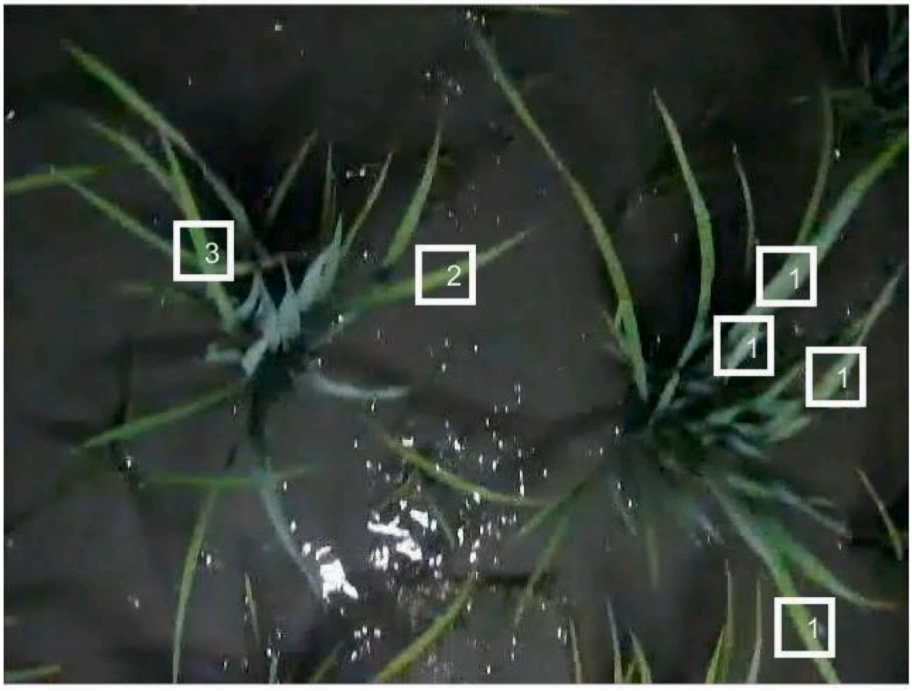

(b)

Fig. 8. Classification results under controlled light conditions (CLC) for the three plant classes: 1) rice plant (R), 2) *Cyperus rotundus* (C) weed, and 3) *Echinochloa* (E) *crus-galli* weed: (a) stereo mode with arithmetic mean (AM) computation, frame extracted from **Arithmetic mean model_CLC.mp4** supplementary video file, and (b) stereo mode with geometric mean (GM) computation, frame extracted from **Geometric mean model_CLC.mp4** supplementary video file.

features to train the classifier. By reviewing previous studies that have used statistical techniques and artificial intelligence-based methods for selecting effective features [42]; Sabzi and Abbaspour Gillandeh, 2018), this study used a neural network with the parameters optimized by a particle swarm optimization algorithm (NN-PSO) to assist the search process and select the most appropriate (effective) features from the entire set of extracted features. PSO is a bio-inspired computational algorithm that works based on randomly selected populations called particle swarms. The PSO algorithm begins by creating a random population. Each component in the population is a different set of decision variables whose optimal value should be satisfied. In fact, each particle represents a vector in the problem-solving space Kennedy [23]. In this

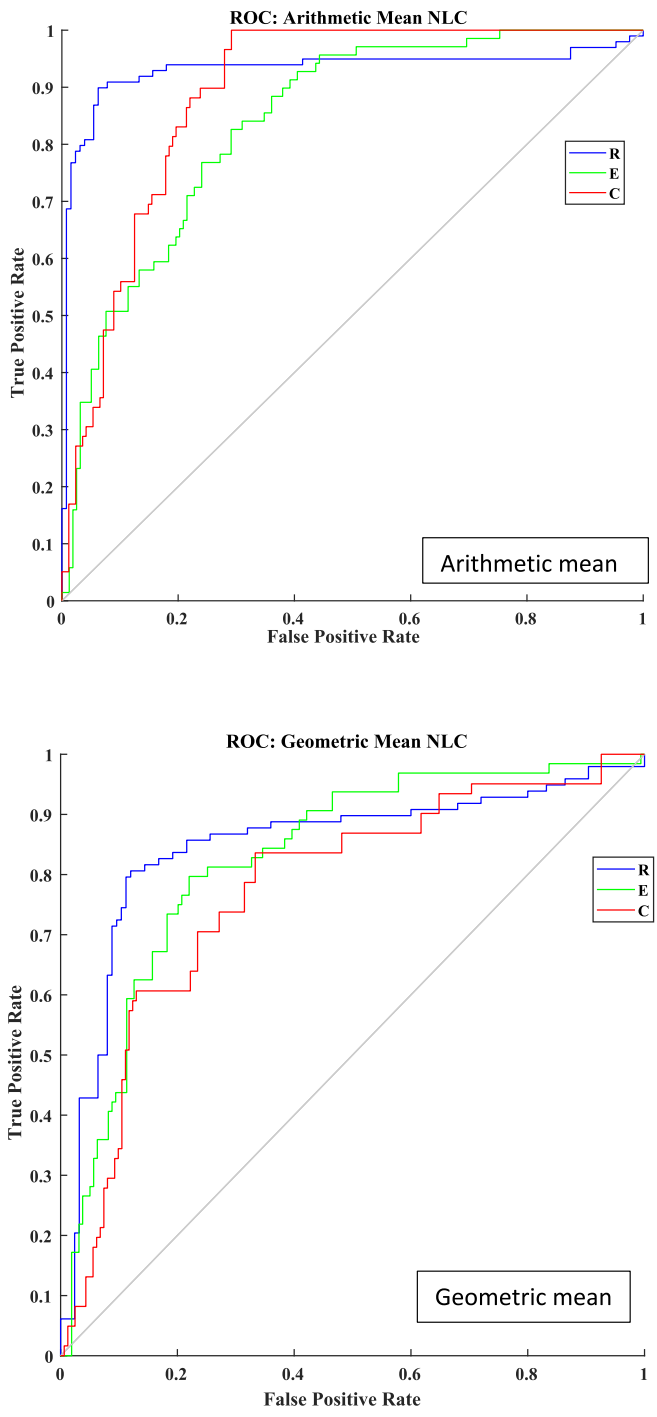

Fig. 9. Performance evaluation of classifier in Arithmetic (AM) [**ROC_Arithmetic mean-natural light.fig**] and Geometric (GM) [**ROC_Geometric mean-natural light.fig**] means based on the ROC curves under natural light conditions (NLC): R = Rice, E = *Echinochloa crus-galli* and C = *Cyperus rotundus* (test set).

algorithm, every action and reaction affects the movement of the group and eventually each member of the group can benefit from the discoveries and skills of the other members. To select the most important features from a total of 302 features extracted by NN-PSO, all the input data samples (objects) extracted from Video frames were divided into training (70 %), validation (15 %), and test (15 %) disjoint data sets. PSO algorithm was used to form feature subsets of different sizes and send them as input data samples at the multilayer perceptron (MLP) neural network.

2.2.4. Classification

Classification systems, such as neural networks, decision tree, nearest neighbor, support vector machines, Bayesian classifier, among others, are used to classify the data. Among them, neural network nonlinear classifiers have more applications due to showing often better performance in developing prediction models and higher accuracy. The present study attempted to use a neural network classifier to discriminate between rice and weeds. To improve the performance of the neural network, a *meta*-heuristic imperialist competitive algorithm (ICA) was used to optimize the network parameters. ICA is a well-known optimization algorithm in the field of evolutionary computation. In fact, if we consider the optimization algorithm as the mathematical equivalence of the biological and natural evolutionary process in nature, this algorithm is equivalent to the mathematical modeling of social evolution. Like other evolutionary algorithms, it starts with a number of random primary populations, each called a country. Some of the best elements of the population are selected as imperialist. The rest of the population is also considered as a colony. The colonies are attracted in dependence on the power of the imperialists. The survival of an empire depends on its ability to attract and dominate the colonies of rival empires (Atashpaz-Gargari and [3]. To classify the objects extracted from images under both imaging conditions (NLC and CLC), a hybrid NN-ICA classifier was used, with different replications. Moreover, to evaluate the performance of the proposed classifier, 70 % of the input data was selected for training the network and the remaining 30 % was selected for testing and validating the classification. The classification results were presented in the form of a table or confusion matrix as one of the commonly accepted valid criteria for evaluating the performance of each classifier in classifying the three different plant classes: Rice, *Echinochloa crus-galli* and *Cyperus rotundus*.

3. Results and discussion

3.1. Extraction of the most effective features using hybrid neural network-particle swarm optimization algorithm (NN-PSO)

The results of using a hybrid combination in NN-PSO to find the six most effective features for both imaging light conditions (NLC and CLC) are shown in Tables 1 and 2, respectively. From a total of 302 extracted features (defined in Table 3), a total of 6 optimal features were selected.

3.2. Ternary (3-class) classification of images

As mentioned earlier, an NN-ICA classifier was used to detect weeds from rice crops. To obtain significant results, the classification process was performed with 100 random replications over train and test sets, under both classification stages. Train set samples must be used only while in the training/learning phase (weight adaption) and never used again when measuring the classification performance, which should be provided with the disjoint (empty intersection) test set, to measure the machine generalization capability to ex-novo test samples.

The results of classification using the NN-ICA classifier for imaging under natural light conditions (NLC) are presented in Tables 4 and 5 in the form of the confusion matrix, for AM and GM, respectively.

Analogous classification results using the NN-ICA classifier for imaging under controlled light conditions (CLC) are presented in Tables 6 and 7 in the form of the confusion matrix, for AM and GM cases, respectively.

As shown in confusion matrices, Tables 4-7, the classification results under CLC have always a higher accuracy than those under NLC, as the classification accuracy for the arithmetic mean was 85.71 % under NLC and 96.95 % under CLC. In addition, the classification accuracy for the geometric mean was 85.63 % under NLC and 94.74 % under CLC. The reason for this difference in recognition accuracy may lie in the effects of ambient light on the quality of images taken on rice field under ambient light conditions and consequently on processing and classification. It can

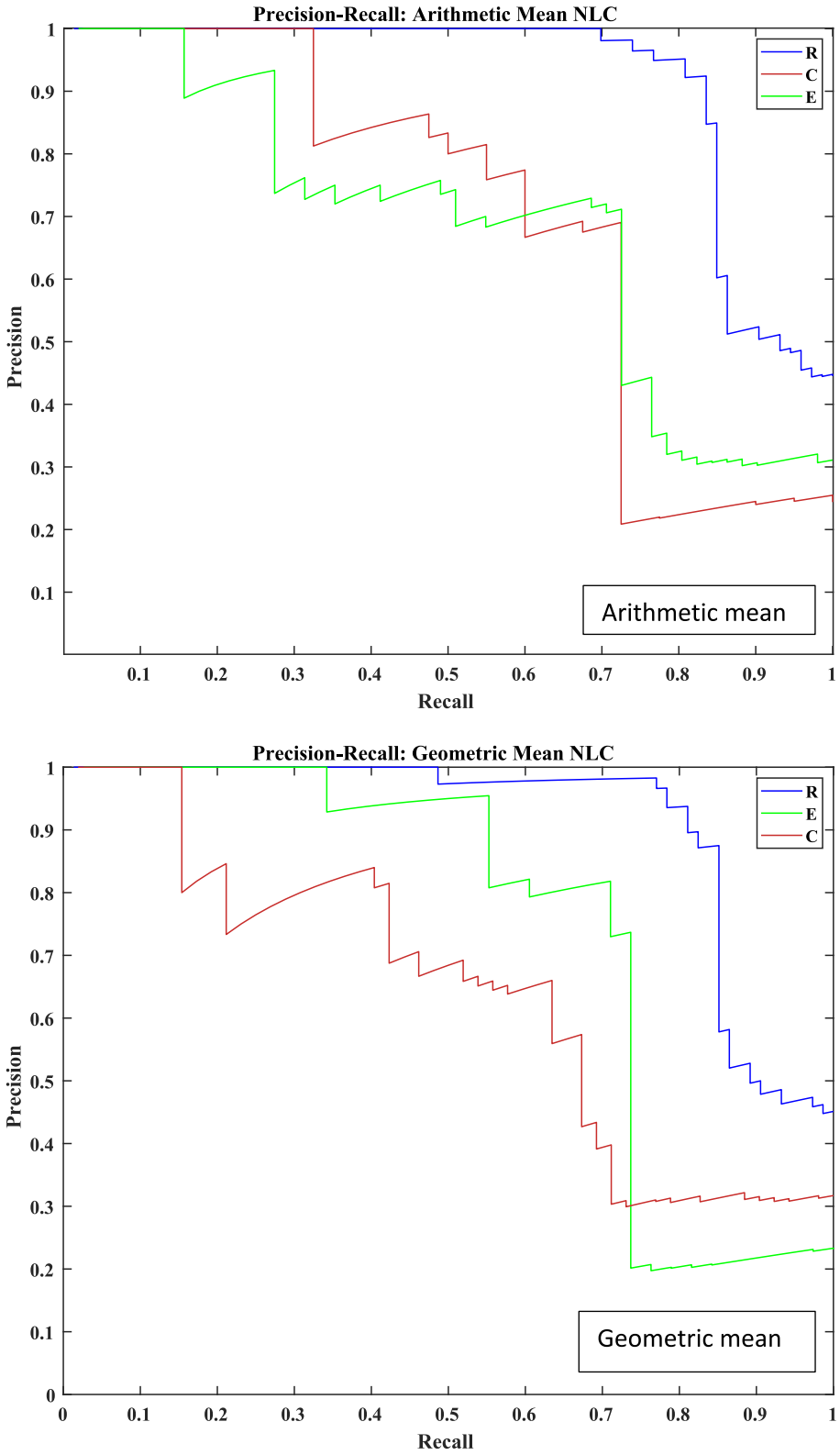

Fig. 10. Performance evaluation of classifier in Arithmetic (AM) [**PR_Arithmetic mean-natural light.fig**] and Geometric (GM) [**PR_Geometric mean-natural light.fig**] means based on the Precision & Recall curves under natural light condition (NLC): R = Rice, E = *Echinochloa crus-galli* and C = *Cyperus rotundus* (test set).

be observed that this system is able to correctly classify all *Cyperus rotundus* weed under controlled light conditions, which is due to the location of occurrence and growth of this type of weed, mainly among the rice plants. Therefore, it was well detected by removing the effects of natural light.

However, because of the close resemblance of *Echinochloa crus-galli* weed with the rice crop and, on the other hand, the possibility of the occurrence and growth of this weed plant even among rice plants, there was some error in recognizing rice over this weed even under controlled light conditions. Also, the classification accuracy including all data by

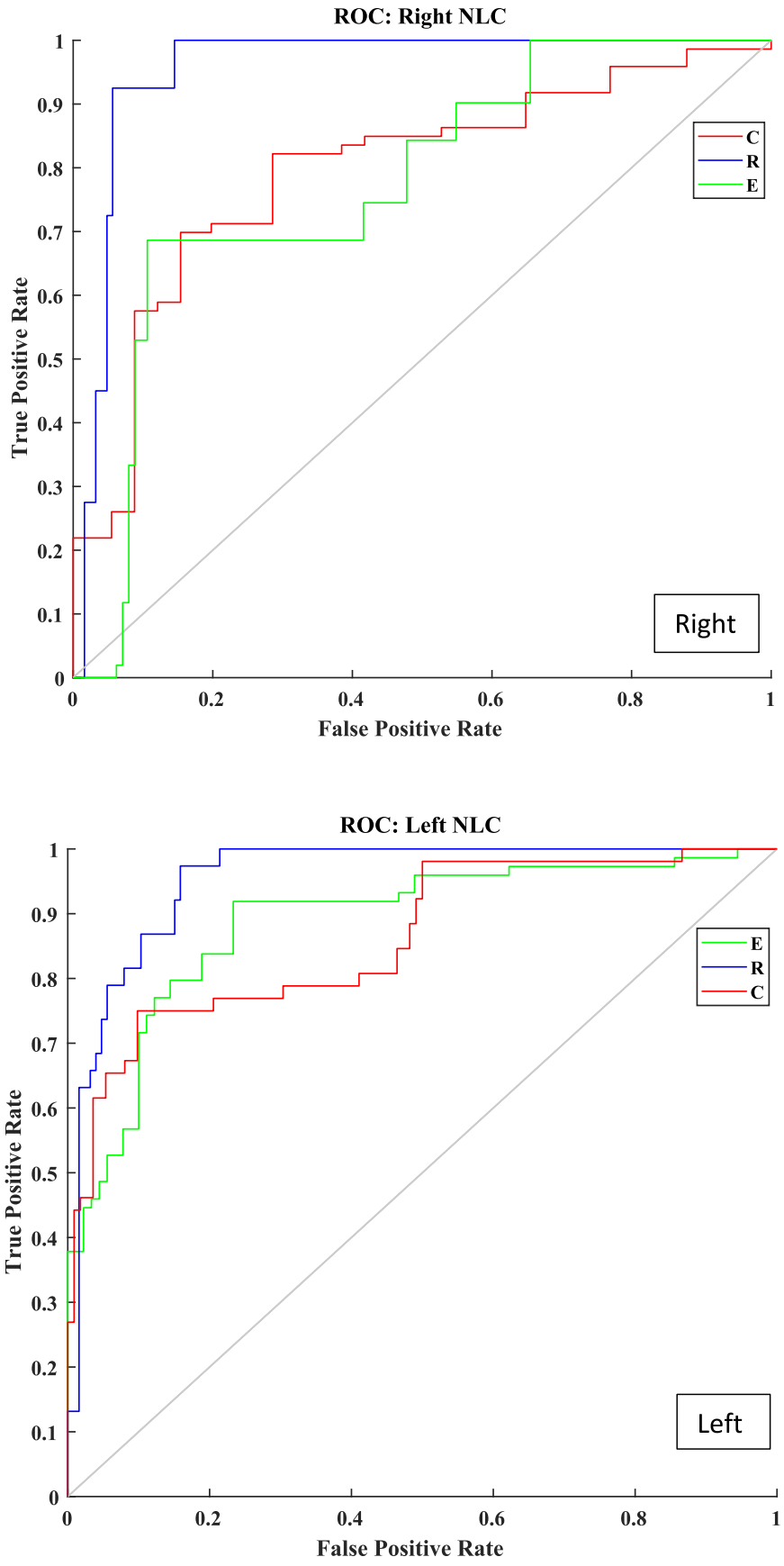

Fig. 11. Performance evaluation of classifier in Right (R) [**ROC_Right channel-natural light.fig**] and Left (L) [**ROC_Left channel-natural light.fig**] channels based on the ROC curves under natural light conditions (NLC): R = Rice, E = *Echinochloa crus-galli* and C = *Cyperus rotundus* (test set).

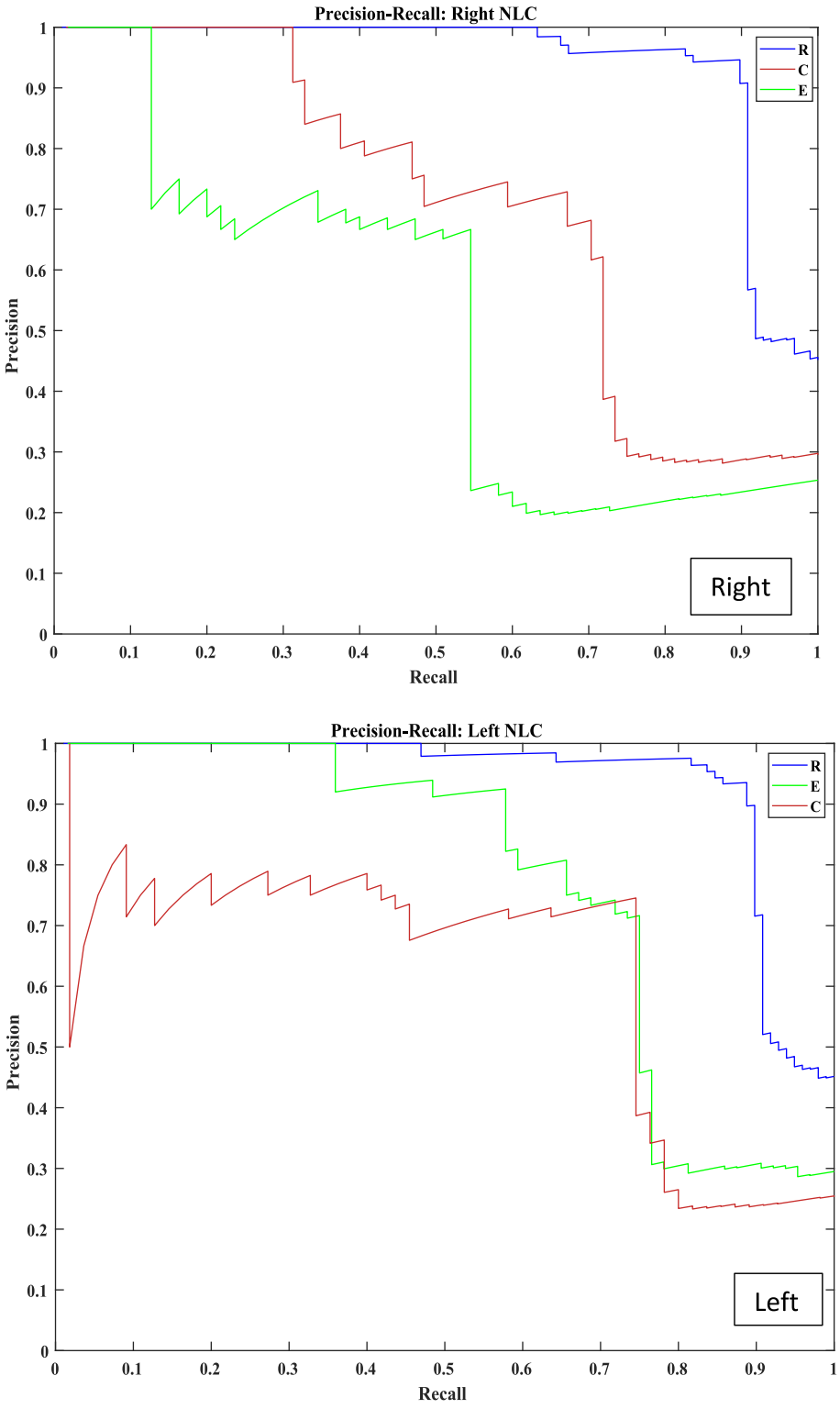

Fig. 12. Performance evaluation of classifier in Right (R) [**PR_Right channel-natural light.fig**] and Left (L) [**PR_Left channel-natural light.fig**] channels based on the Precision & Recall curves under natural light conditions (NLC): R = Rice, E = *Echinochloa crus-galli* and C = *Cyperus rotundus* (test set).

the arithmetic mean was always higher than that done by geometric mean, which is consistent with Dadashzadeh et al. [10].

To investigate the performance of the proposed stereoscopic vision method in discriminating rice from weeds, the processing and classification results for each camera channel for controlled light conditions are presented separately in Tables 8 and 9, for the L and R channels, respectively.

It can be seen that the classification accuracy in the stereo imaging mode is higher than the classification accuracy in the single-channel processing mode, as expected, which is due to the full coverage of field details when stereoscopic vision is used. Classification results are shown for several example frames for natural light conditions in Fig. 7 and for controlled light conditions in Fig. 8.

Since the proposed method is new, an attempt was made to compare

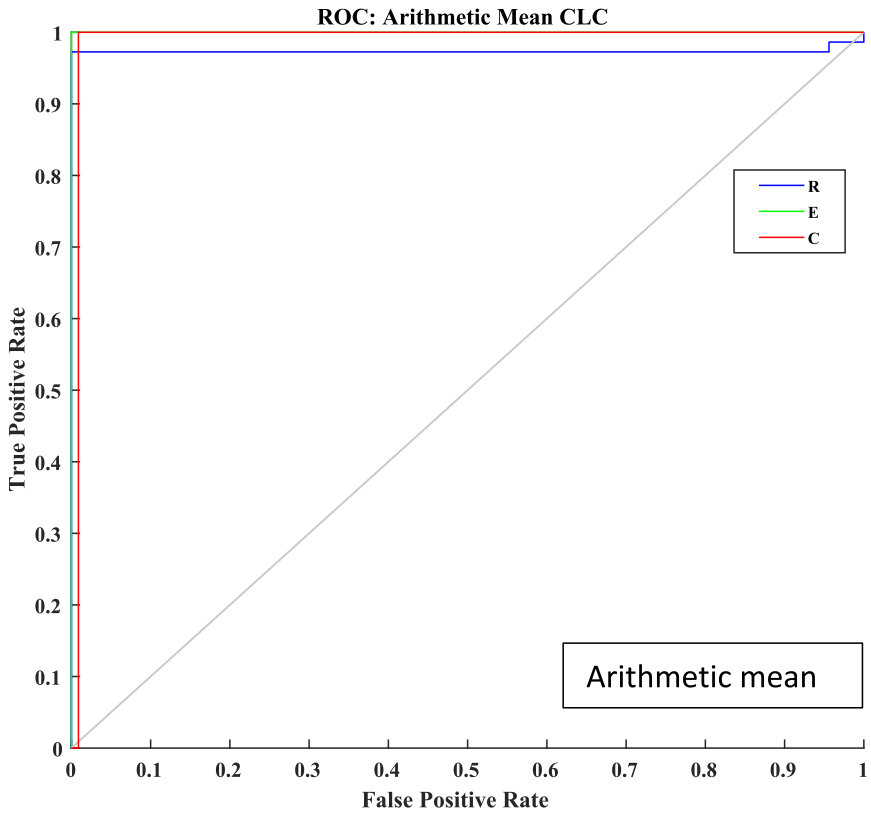

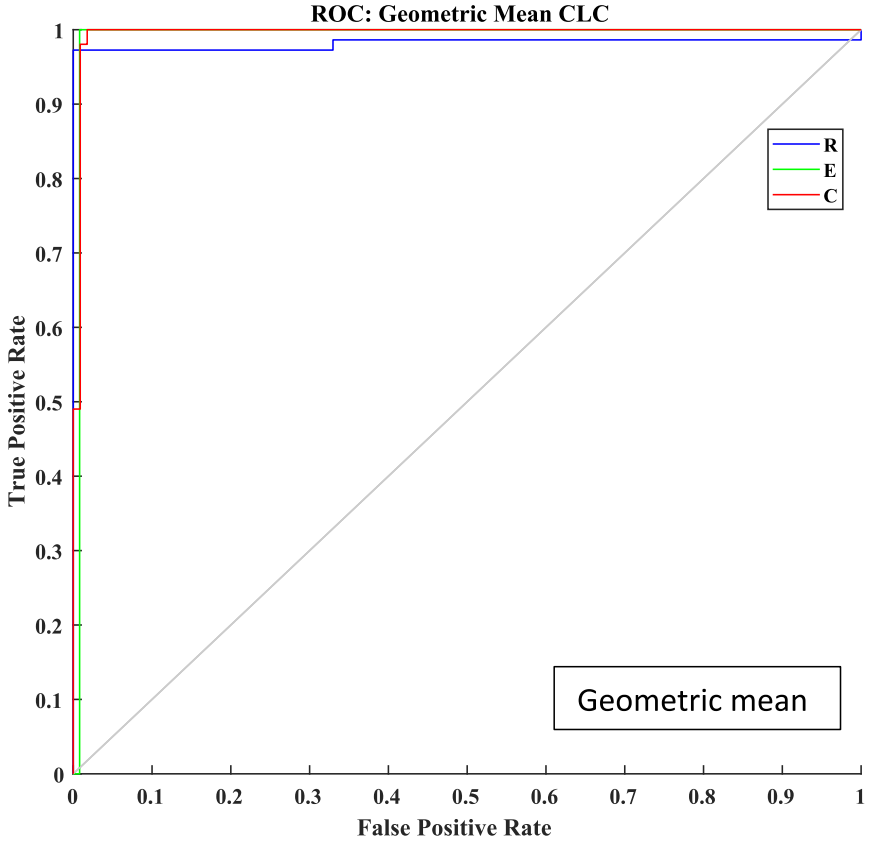

Fig. 13. Performance evaluation of classifier in Arithmetic (AM) [**ROC_Arithmetic mean-controlled light.fig**] and Geometric (GM) [**ROC_Geometric mean-controlled light.fig**] means based on the ROC curves in controlled light conditions (CLC): R = Rice, E = *Echinochloa crus-galli* and C = *Cyperus rotundus* (test set).

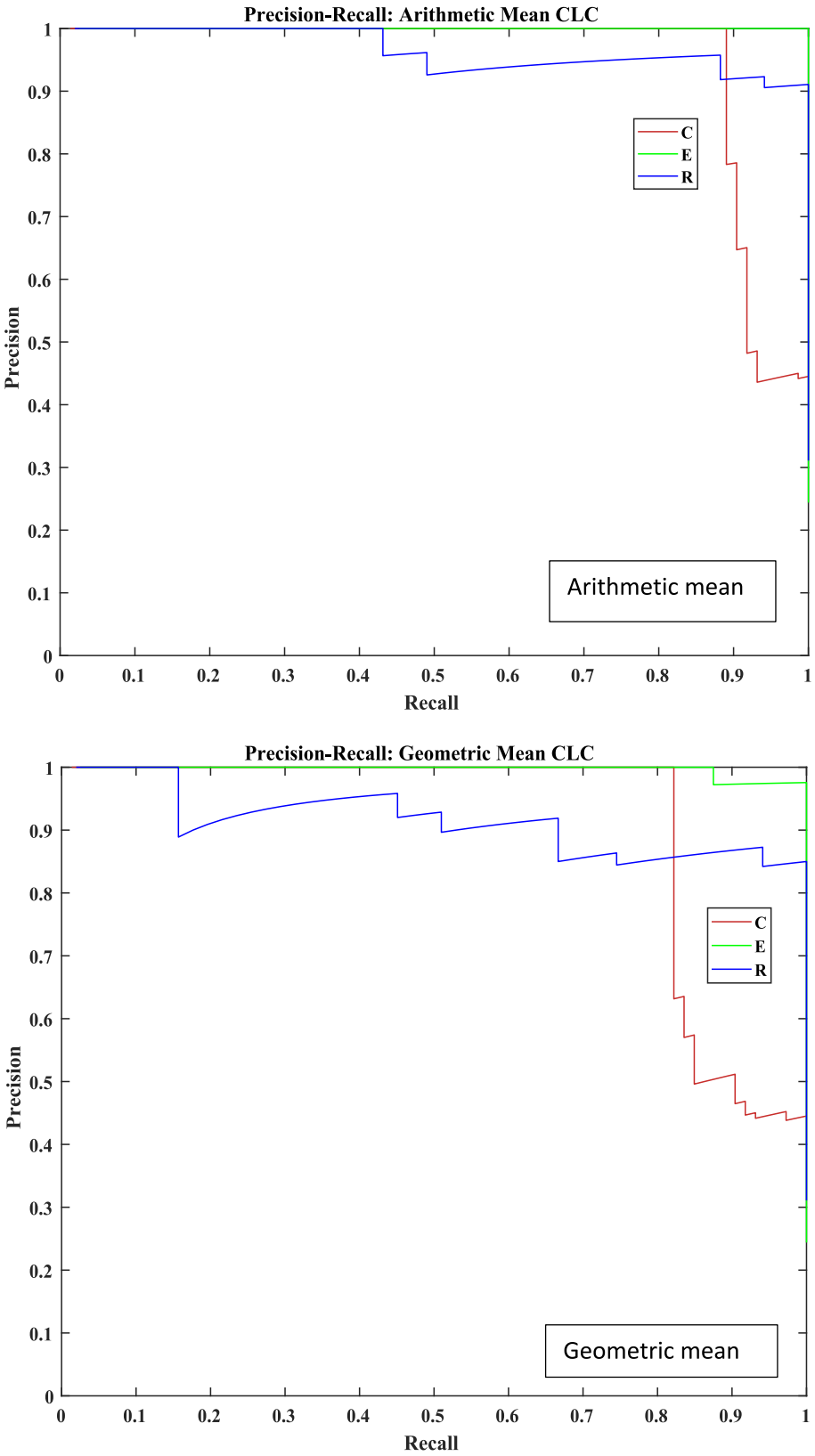

Fig. 14. Performance evaluation of classifier in Arithmetic (AM) [**PR_Arithmetic mean-controlled light.fig**] and Geometric (GM) [**PR_Geometric mean-controlled light.fig**] means based on the Precision & Recall curves under controlled light conditions (CLC): R = Rice, E = *Echinochloa crus-galli* and C = *Cyperus rotundus* (test set).

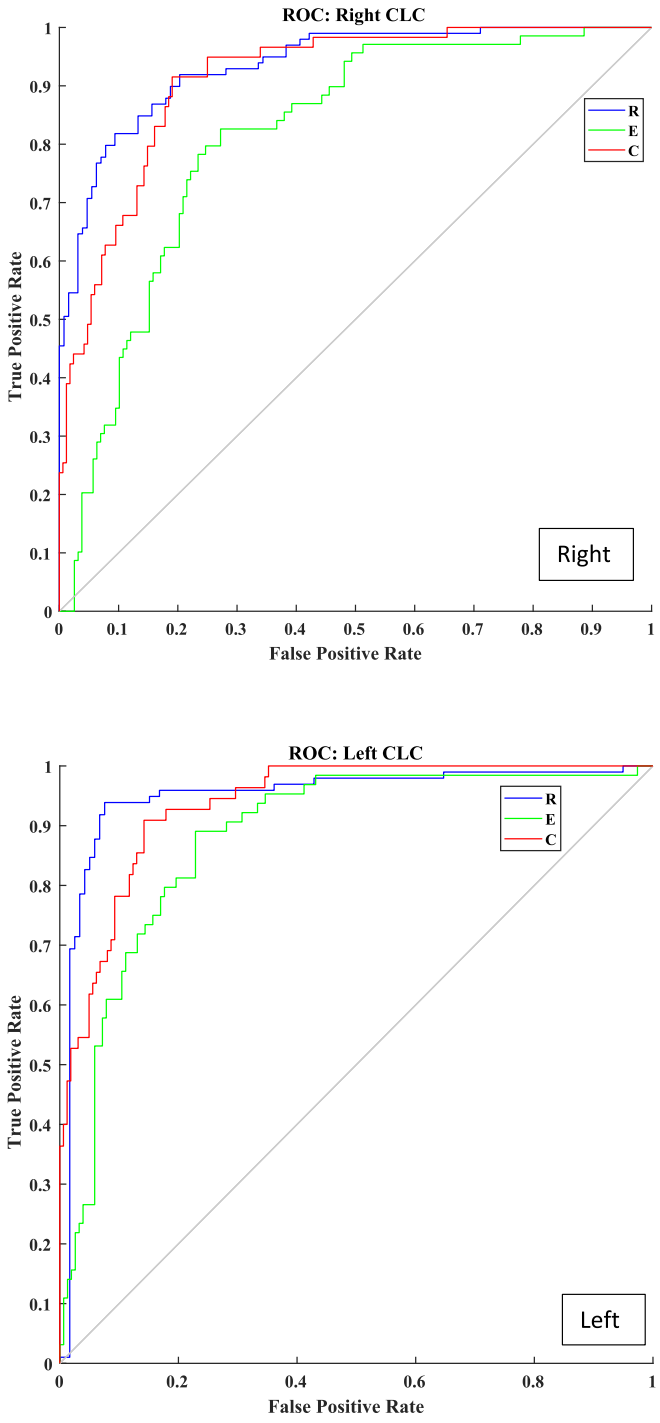

Fig. 15. Performance evaluation of classifier in Right (R) [**ROC_Right channel-controlled light.fig**] and Left (L) [**ROC_Left channel-controlled light.fig**] channels based on the ROC curves under controlled light conditions (CLC): R = Rice, E = *Echinochloa crus-galli* and C = *Cyperus rotundus* (test set).

the results with those of similar works. In a study conducted by Jin and Tang [19], it was stated that although there are some 2D vision-based systems for sensing corn plants in the early growth stages, some of the shortcomings are difficult to overcome. The biggest challenge is to separate corn plants on field that overlap with other plants.

When using 2D vision, the outdoors changing light conditions and the presence of weeds in the background may cause problems in detecting corn plants. Thus, adding depth information can improve the performance of such a system. Therefore, a new corn plant sensing system was investigated using a real-time stereo vision.

The experimental results showed that the stereo vision system correctly detected 96.7 % of corn plants during field experiment. However, the type of plant, canopy structure, and field conditions are different from those of rice plant. In another study, Ashrafa and Niaz Khan [2] presented two classification methods for weed detection in rice fields based on grass density.

The first method used the texture features extracted from the gray level co-occurrence matrix (GLCM). They achieved 73 % accuracy in the detection of rice from umbrella sedge weed by using Radial basis function (RBF) NN and support vector machine (SVM). The second method used features such as shape and anatomy, which are stable in scale and rotation, for classification based on grass density. The second technique achieved an 86 % accuracy using a random forest classifier, which resulted better than first technique. Although only nutgrass and rice were present in the images in this study and the aim was to separate both plants, results were less accurate (since different dataset used, one needs to be cautious here) than the *meta*-heuristic algorithm proposed in the present study.

3.3. *Evaluation and comparison of classifiers performance using both ROC and precision- recall (PR) curves AUC*

ROC curve analysis and ROC-Area Under Curve (AUC) computation is very desirable whenever the cost (penalty) associated to either type I (false positive, FP) or type II (false negative, FN) classification errors are not known, since in that case one cannot define and fix an optimal classifier working point, and there is need to evaluate how the classifier performs over the $\{\text{FP rate}, \text{TP rate}\}$ or equivalently $\{1-\text{specificity}, \text{sensitivity}\}$ plane by slowly varying the output classifier detection threshold and computing both FPR and TPR fraction values, for each and every classifier output detection threshold fixed values.

ROC curve analysis is often used to evaluate the performance of classification algorithms, especially in the case of binary classification problems in supervised machine learning, despite it can be easily extended to multi-class problems.

For this reason, ROC curves might be used to evaluate the performance of the classifiers in this research. However, when dealing with highly skewed and/or imbalanced datasets, Precision & Recall (PR) curves provide a complimentary picture of the performance of an algorithm, together with ROC curves. Therefore, PR curves were also used to evaluate the performance of the classifiers and the AUC value of all three classes were computed under both ROC and precision-recall curves, called ROC-AUC and PR-AUC.

Figs. 9 to 16 show the ROC and precision-recall curves for different imaging conditions, and Tables 10 and 11 show the computed AUC values for the ROC and precision-recall curves, all test set. In summary, the results showed that for the problem in hand, compared to the PR curves, the ROC curves had a very good and stable property in showing the performance of the classifiers, while the PR curves showed slightly more inconsistent AUC computed values. ROC curve allows us to minimize misclassifications from different classes and to measure model performance in a more objective way.

The computed AUC values show that the classifiers performed better in classifying the classes under controlled light conditions (CLC) as compared to natural light conditions (NLC), as expected. Also, the performance of the classifiers in stereo (3D) imaging mode have been more favorable than corresponding 2D imaging modes, also as expected, given the additional information available coming from the two independent camera image sources.

4. Conclusion

The present study investigated a new technique for using stereo vision to detect and classify rice crops from weeds in-field under two imaging light conditions, either NLC or CLC. For this purpose, various

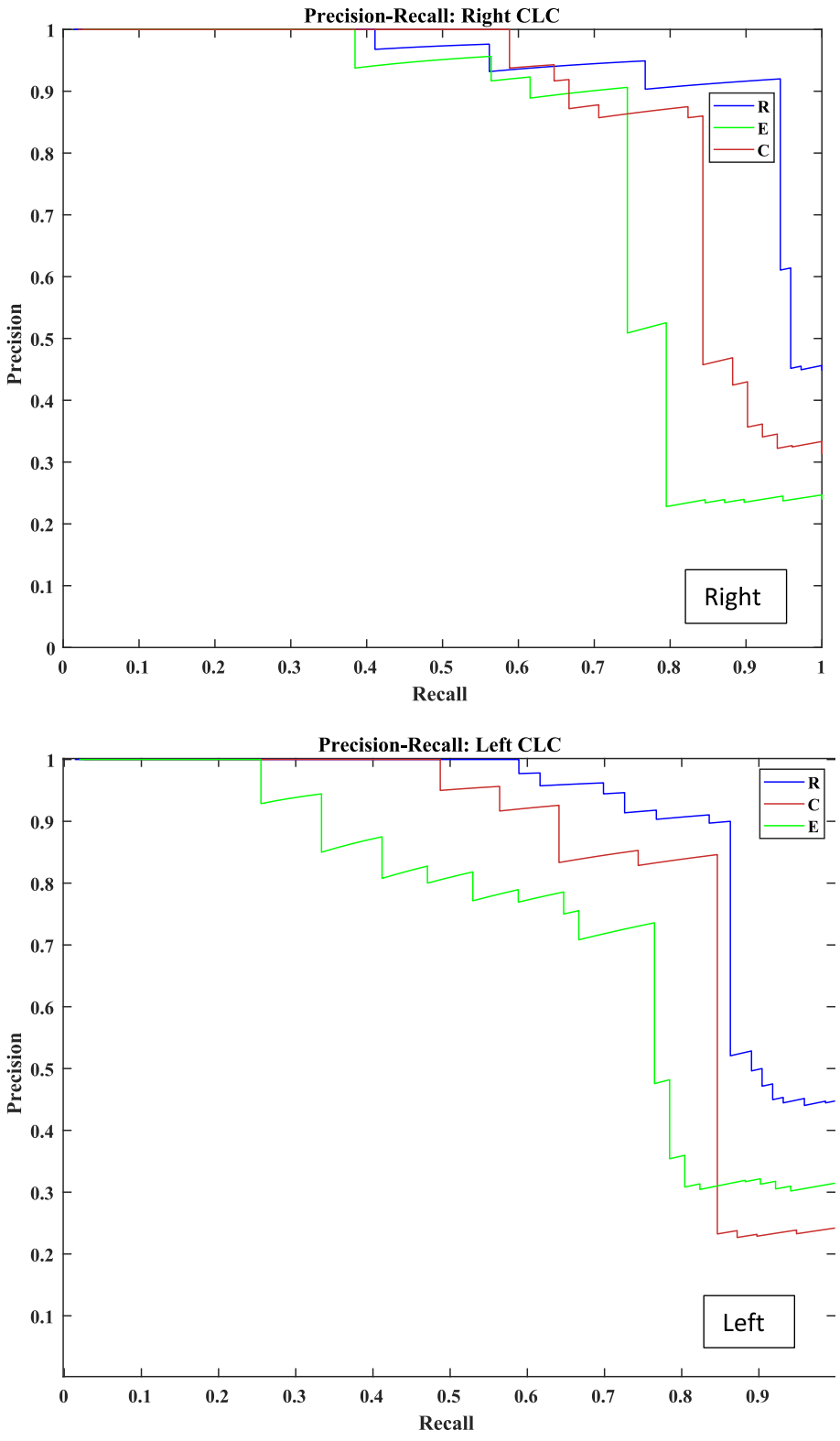

Fig. 16. Performance evaluation of classifier in Right (R) [**PR_Right channel-controlled light.fig**] and Left (L) [**PR_Left channel-controlled light.fig**] channels based on the Precision & Recall curves under controlled light conditions (CLC): R = Rice, E = *Echinochloa crus-galli* and C = *Cyperus rotundus*.

Videos from rice field were taken and processed under both natural and controlled light conditions. To classify and recognize crop from weeds, detection and feature extraction from the objects extracted from the images were performed after separating frames related to the right (R) and left (L) channels of the stereoscopic camera. Then, the corresponding pixels between the right (R) and left (L) channels were selected and mean values were computed. To achieve high accuracy in classification, a hybrid *meta*-heuristic neural network-particle swarm optimization (NN-PSO) algorithm was used to select the effective features and a hybrid neural network-imperialist competitive (NN-ICA) algorithm was used for classification under both imaging light conditions. Results showed that the discrimination of crop and weeds with images under

Table 10
ROC-AUC and Precision & Recall-AUC values in natural light condition (NLC): test set.

Natural Light Condition (NLC)	ROC-AUC			Precision & Recall-AUC		
Class	**Rice**	***Cyperus rotundus***	***Echinochloa crus-galli***	**Rice**	***Cyperus rotundus***	***Echinochloa crus-galli***
Arithmetic mean (AM)	0.9139	0.8806	0.8656	0.9019	0.8551	0.8312
Geometric mean (GM)	0.9022	0.8647	0.8988	0.9154	0.8223	0.8561
Right channel (R)	0.9348	0.8611	0.8586	0.9414	0.8501	0.8104
Left channel (L)	0.9252	0.8436	0.8754	0.9356	0.8175	0.8560

Table 11
ROC-AUC and Precision & Recall-AUC values in controlled light condition (CLC): test set.

Controlled light Condition (CLC)	ROC-AUC			Precision & Recall-AUC		
Class	**Rice**	***Cyperus rotundus***	***Echinochloa crus-galli***	**Rice**	***Cyperus rotundus***	***Echinochloa crus-galli***
Arithmetic mean (AM)	0.9914	1.0000	1.0000	0.9672	0.9575	1.0000
Geometric mean (GM)	0.9982	0.9995	1.0000	0.8913	0.9324	0.9841
Right channel (R)	0.9152	0.8992	0.8511	0.9085	0.8848	0.8568
Left channel (L)	0.9114	0.8971	0.8723	0.9057	0.8727	0.8514

CLC was consistently more accurate than the classification with the images taken under NLC, as expected. In addition, the classification accuracy using the proposed stereoscopic method is higher than the classification accuracy using the images taken by a conventional single source camera. Future research work may focus on investigating the performance of the proposed method in different crop varieties and other weeds.

We believe that the main limitation of our approach has to do with the high variability of weed and plants that could exist in different crop fields, even in different rice fields around the globe, both in terms of weed species and sub-species and in the amount/size of extension or growth stage of weed species as compared to crop/rice plants for a given weed detection period of time.

Even so, given the high accuracy (low error rates) achieved results, we are expecting that the process of weed detection and classification will not suffer a very severe decrease in performance and thus still be helpful in most rice fields under most growing stages.

CRediT authorship contribution statement

Mojtaba Dadashzadeh: Writing – original draft, Resources, Formal analysis, Data curation, Conceptualization. **Yousef Abbaspour-Gilandeh:** Writing – review & editing, Validation, Supervision, Project administration, Funding acquisition, Investigation, Resources. **Tarahom Mesri-Gundoshmian:** Software, Resources, Methodology. **Sajad Sabzi:** Visualization, Software, Investigation, Data curation, Conceptualization. **Juan Ignacio Arribas:** Writing – review & editing, Validation, Methodology, Funding acquisition, Conceptualization, Formal analysis, Visualization.

Declaration of competing interest

The authors declare that they have no known competing financial interests or personal relationships that could have appeared to influence the work reported in this paper.

Data availability

Data will be made available on request.

Acknowledgments

J. I. Arribas wants to thank the Spanish Ministry for Science, Innovation and Universities (MICINN), Agencia Estatal de Investigacion (AEI), as well as to the Fondo Europeo de Desarrollo Regional funds (FEDER, EU), under grant number PID2021-122210OB-I00, by MCIN/AEI/10.13039/501100011033 and "ERDF A way of making Europe", European Union, for partially funding this work.

Appendix A. Supplementary materials

A1 Supplementary ROC and precision-recall (PR) classification curves in MatLab .fig source figure file format for both NLC and CLC light conditions from Section 3.3

For reproducible purposes, we provide next the MatLab .fig classification performance source figure files for both ROC and precision-recall (PR) curves for GM, AM, R, and L channels, and under both NLC and CLC lighting conditions, extracted from Section 3.3:

Figure 9: ROC_Arithmetic mean-natural light.fig, ROC_Geometric mean-natural light.fig

Figure 10: PR_Arithmetic mean-natural light.fig, PR_Geometric mean-natural light.fig

Figure 11: ROC_Right channel-natural light.fig, ROC_Left channel-natural light.fig

Figure 12: PR_Right channel-natural light.fig, PR_Left channel-natural light.fig

Figure 13: ROC_Arithmetic mean-controlled light.fig, ROC_Geometric mean-controlled light.fig

Figure 14: PR_Arithmetic mean-controlled light.fig, PR_Geometric mean-controlled light.fig

Figure 15: ROC_Right channel-controlled light.fig, ROC_Left channel-controlled light.fig

Figure 16: PR_Right channel-controlled light.fig, PR_Left channel-controlled light.fig

A2 Supplementary original and detected video models in .mp4 file format under both NLC and CLC light conditions

For reproducible purposes, we share a total of 12 .mp4 supplementary video (SV) files, both including weed detected and original (no detection) camera recordings, with a Fujifilm FinePix Real 3D-W3 stereo video camera (Tokyo, Japan) equipped with a 10-megapixel CCD sensor recording stereo videos (NTSC, ISO 400 sensitivity, frame resolution of 480×440 pixels, 30 fps), as detailed next:

Natural light conditions (NLC): Arithmetic mean (Arithmetic mean model_NLC.mp4) Geometric mean (Geometric mean model_NLC.mp4), Right (Right channel model_NLC.mp4) and Left (Left channel model_NLC.mp4) channels weed detected videos, together with

original R (SV_NLC_ORIG_R.mp4) and L (SV_NLC_ORIG_L.mp4) channel recordings (undetected).
Controlled light conditions (CLC): Arithmetic mean (Arithmetic mean model_CLC.mp4) Geometric mean (Geometric mean model_CLC.mp4), Right (Right channel model_CLC.mp4) and Left (Left channel model_CLC.mp4) channels weed detected videos, together with original R (SV_CLC_ORIG_R.mp4) and L (SV_CLC_ORIG_L.mp4) channel recordings (undetected).

Note: original AVI video format recordings were converted to .mp4 video format for further processing with MatLab software and toolboxes (Mathworks, Natick, MA).

Appendix B. Supplementary material

Supplementary material to this article can be found online at https://doi.org/10.1016/j.measurement.2024.115072.

References

[1] H.J. Andersen, L. Reng, K. Kirk, Geometric plant properties by relaxed stereo vision using simulated annealing, Comput. Electron. Agric. 49 (2) (2005) 219–232.
[2] T. Ashrafa, Y. Niaz Khan, Weed density classification in rice crop using computer vision, Comput. Electron. Agric. 175 (2020) 105590.
[3] E. Atashpaz-Gargari, C. Lucas, Imperialist competitive algorithm: an algorithm for optimization inspired by imperialistic competition, IEEE Congress on Evolutionary Computation (2007) 4661–4667.
[4] X. Bai, Z. Cao, Y. Wang, Z. Yu, Z. Hu, X. Zhang, C. Li, Vegetation segmentation robust to illumination variations based on clustering and morphology modelling, Biosyst. Eng. 125 (2014) 80–97.
[5] B. Biskup, H. Scharr, U. Schurr, U. Rascher, A stereo imaging system for measuring structural parameters of plant canopies, Plant Cell Environ. 30 (10) (2007) 1299–1308.
[6] S. Bordoloi, V. Kashyap, A. Garg, S. Sreedeep, L. Wei, S. Andriyas, Measurement of mechanical characteristics of fiber from a novel invasive weed: a comprehensive comparison with fibers from agricultural crops, Measurement 113 (2018) 62–70.
[7] X.P. Burgos-Artizzua, A. Ribeiroa, M. Guijarrob, G. Pajares, Real-time image processing for crop/weed discrimination in maize fields, Comput. Electron. Agric. 75 (2011) 337–346.
[8] M. Carrara, A. Comparetti, P. Febo, S. Orlando, Spatially variable herbicide application on durum wheat in sicily, Biosyst. Eng. 87 (4) (2004) 387–392.
[9] S. Dandrifosse, A. Bouvry, V. Leemans, B. Dumont, B. Mercatoris1, Imaging wheat canopy through stereo vision: overcoming the challenges of the laboratory to field yransition for morphological features extraction, Front. Plant Sci. 11 (2020) 96.
[10] M. Dadashzadeh, Y. Abbaspour-Gilandeh, T. Mesri-Gundoshmian, S. Sabzi, J. L. Hernández-Hernández, M. Hernández-Hernández, J.I. Arribas, Weed classification for site-specific weed management using an automated stereo computer-vision machine-learning system in rice fields, Plants 9 (5) (2020) 559.
[11] G. Dhingra, V. Kumar, H.D. Joshi, A novel computer vision based neutrosophic approach for leaf disease identification and classification, Measurement 135 (2019) 782–794.
[12] M.A. Dickson, W.C. Bausch, M.S. Howarth, Classification of a broadleaf weed, a grassy weed and corn using image processing techniques, Proc. SPIE 2345 (1995) 297–305.
[13] K. Dutta, D. Talukdar, S.S. Bora, Segmentation of unhealthy leaves in cruciferous crops for early disease detection using vegetative indices and Otsu thresholding of aerial images, Measurement 189 (2022) 110478.
[14] T.Y. Goh, S.N. Basah, H. Yazid, M.J.A. Safar, F.S.A. Saad, Performance analysis of image thresholding: otsu technique, Measurement 114 (2018) 298–307.
[15] S. Hameed I. Amin Detection of weed and wheat using image processing 2018 IEEE International Conference on Engineering Technologies & Applied Sciences 2018 Bangkok Thailand 22–23.
[16] E. Hamuda, B. Mc-Ginley, M. Glavin, E. Jones, Automatic crop detection under field conditions using the HSV colour space and morphological operations, Comput. Electron. Agric. 133 (2017) 97–107.
[17] A.S.M.M. Hasan, F. Sohel, D. Diepeveen, H. Laga, M.G.K. Jones, A survey of deep learning techniques for weed detection from images, Comput. Electron. Agric. 184 (2021) 106067.
[18] B. Jamshidi, E. Mohajerani, J. Jamshidi, Developing a Vis/NIR spectroscopic system for fast and non-destructive pesticide residue monitoring in agricultural product, Measurement 89 (2016) 1–6.
[19] T. Jin, L. Tang, Corn plant sensing using real-time stereo vision, J. Field Rob. 26 (6–7) (2009) 591–608.
[20] R. Kamath, M. Balachandra, A. Vardhan, U. Maheshwari, Classification of paddy crop and weeds using semantic segmentation, Cogent Engineering 9 (2022) 2018791.
[21] A. Kamilaris, F.X. Prenafeta-Boldú, Deep learning in agriculture: a survey, Comput. Electron. Agric. 147 (2018) 70–90.
[22] I. Kansal, V. Khullar, J. Verma, R. Popli, R. Kumar, IoT-Fog-enabled robotics-based robust classification of hazy and normal season agricultural images for weed detection, J. Behav. Robot. 14 (2023) 20220105.
[23] Kennedy, J. & R. Eberhart, 1995. Particle Swarm Optimization. Paper presented at Proceedings of the IEEE International Conference on Neural Networks, Perth, Australia.
[24] J. Li, L. Tang, Crop recognition under weedy conditions based on 3D imaging for robotic weed control, J. Field Robotics. (2017) 1–16.
[25] Lin, C., 2009. A Support Vector Machine Embedded Weed Identification System, thesis, Submitted in partial fulfillment of the requirements for the degree of Master of Science in Agricultural Engineering in the Graduate College of the University of Illinois at Urbana-Champaign.
[26] G.E. Meyer, J.C. Neto, D.D. Jones, T.W. Hindman, Intensified fuzzy clusters for classifying plant, soil, and residue regions of interest from color images, Comput. Electron. Agric. 42 (3) (2003) 161–180.
[27] W.M. Miller, A.W. Schumann, J.D. Whitney, S. Buchanon, Variable rate application of granular fertilizer for citrus test plots, Appl. Eng. Agri. 21 (5) (2005) 795–801.
[28] M. Müller-Linow, F. Pinto-Espinosa, H. Scharr, U. Rascher, The leaf angle distribution of natural plant populations: assessing the canopy with a novel software tool, Plant Methods 11 (1) (2015) 1–16.
[29] A. Paikekari, V. Ghule, R. Meshram, V.B. Raskar, Weed detection using image processing, Int. Res. J. Eng. Technol. 3 (3) (2016) 1220–1222.
[30] H. Rahimikhoob, M. Delshad, R. Habibi, Leaf area estimation in lettuce: comparison of artificial intelligence-based methods with image analysis technique, Measurement 222 (2023) 113636.
[31] K. Sabanci, C. Aydin, Smart robotic weed control system for sugar beet, J. Agric. Sci. Technol. 19 (2017) 73–83.
[32] S. Sabzi, Y. Abbaspour-Gilandeh, using video processing to classify potato plant and three types of weed using hybrid of artificial neural network and particle swarm algorithm, Measurement 126 (2018) 22–36.
[33] S. Sabzi, Y. Abbaspour-Gilandeh, G. Garcia-Mateos, A fast and accurate expert system for weed identification in potato crops using metaheuristic algorithms, Comput. Ind. 98 (2018) 80–89.
[34] A.W. Schumann, W.M. Miller, Q.U. Zaman, K. Hostler, S. Buchanon, S. Cugati, Variable rate granular fertilization of citrus groves: spreader performance with single-tree prescription zones, Appl. Eng. Agric. 22 (1) (2006) 19–24.
[35] M. Siddiqi, S. Lee, A. Khan, Weed image classification using wavelet transform, stepwise linear discriminant analysis and support vector machines for an automatic spray control system, J. Inf. Sci. Eng. 30 (2014) 1253–1270.
[36] D.C. Slaughter, D.K. Giles, D. Downey, Autonomous robotic weed control systems: a review, Comput. Electron. Agric. 6 (1) (2008) 63–78.
[37] J. Sun, J. Zhou, Y. Wang, Y. He, H. Jia, A cutting width measurement method for the unmanned rice harvester based on RGB-D images, Measurement 224 (2024) 113777.
[38] J. Tang, X.Q. Chen, R.H. Miao, D. Wang, Weed detection using image processing under different illumination for site-specific areas spraying, Comput. Electron. Agric. 122 (2016) 103–111.
[39] V.K. Tewari, A.A. Kumar, B. Nare, S. Prakash, A. Tyagi, Microcontroller based roller contact type herbicide applicator for weed control under row crops, Comput. Electron. Agric. 104 (2014) 40–45.
[40] A. Wang, W. Zhang, X. Wei, A review on weed detection using ground-based machine vision and image processing techniques, Comput. Electron. Agric. 158 (2019) 226–240.
[41] J. Wang, Y. Zhang, R. Gu, Research status and prospects on plant canopy structure measurement using visual sensors based on three-dimensional reconstruction, Agriculture 10 (2020) 462.
[42] M. Weis, M. Sokefeld, Detection and Identification of Weeds, in: Precision Crop Protection - the Challenge and Use of Heterogeneity, Springer, Netherlands, 2010, pp. 119–134.
[43] Z. Wu, Y. Chen, B. Zhao, Review of weed detection methods based on computer vision, Sensors 21 (2021) 3647.
[44] W. Yang, S. Wang, X. Zhao, J. Zhang, J. Feng, Greenness identification based on HSV decision tree, Inform. Proc. Agri. 2 (3–4) (2015) 149–160.
[45] M. Yong, M. Warshauer, Arithmetic and geometric mean, Menemui. Mat. 24 (2) (2002) 17–22.
[46] Young, D., S. Miller., H. Fisher & M. Shenk, 2017. Selecting Appropriate Weed Control Systems for Developing Countries. (Press), Published by: Weed Science Society of America and Allen Press Stable, 26(3):209–212.
[47] Q.U. Zamana, T.J. Esaua, A.W. Schumannb, D.C. Percivalc, Y.K. Changa, S. M. Reada, A.A. Farooquea, Development of prototype automated variable rate sprayer for real-time spot-application of agrochemicals in wild blueberry fields, Comput. Electron. Agri. 76 (2011) 175–182.
[48] H. Zareiforoush, S. Minaei, M.R. Alizadeh, A. Banakar, A hybrid intelligent approach based on computer vision and fuzzy logic for quality measurement of milled rice, Measurement 66 (2015) 26–34.
[49] N. Zhao, L. Zhou, T. Huang, M.F. Taha, Y. He, Z. Qiu, Development of an automatic pest monitoring system using a deep learning model of DPeNet, Measurement 203 (2022) 111970.